On the stoichiometry of Deinococcus radiodurans Dps-1 binding to duplex DNA

ARTICLE *in* PROTEINS STRUCTURE FUNCTION AND BIOINFORMATICS · MARCH 2012

Impact Factor: 2.63 · DOI: 10.1002/prot.23228 · Source: PubMed

PROTEINS
STRUCTURE ■ FUNCTION ■ BIOINFORMATICS

On the stoichiometry of *Deinococcus radiodurans* Dps-1 binding to duplex DNA

Khoa H. Nguyen, Luke T. Smith, LiJuan Xiao, Gargi Bhattacharyya, and Anne Grove*

Department of Biological Sciences, Louisiana State University, Baton Rouge, Louisiana 70803

ABSTRACT

DNA protection during starvation (Dps) proteins, dodecameric assemblies of four-helix bundle subunits, contribute to protection against reactive oxygen species. *Deinococcus radiodurans*, which is characterized by resistance to DNA damaging agents, encodes two Dps homologs, of which Dps-1 binds DNA with high affinity. DNA binding requires N-terminal extensions preceding the four-helix bundle core. Composed of six Dps-1 dimers, each capable of DNA binding by N-terminal extensions interacting in consecutive DNA major grooves, dodecameric Dps-1 would be predicted to feature six DNA binding sites. Using electrophoretic mobility shift assays and intrinsic tryptophan fluorescence, we show that dodecameric Dps-1 binds 22-bp DNA with a stoichiometry of 1:6, consistent with the existence of six DNA binding sites. The stoichiometry of Dps-1 binding to 26-bp DNA is 1:4, suggesting that two Dps-1 dodecamers can simultaneously occupy opposite faces of this DNA. Mutagenesis of an arginine (Arg132) on the surface of Dps-1 leads to a reduction in DNA binding. Altogether, our data suggest that duplex DNA lies along the dimer interface, interacting with Arg132 and the N-terminal α-helices, and they extend the hexagonal packing model for Dps–DNA assemblies by specifying the basis for occupancy of available DNA binding sites.

Proteins 2012; 80:713–721.

Key words: Dps; electrophoretic mobility shift assay; DNA binding; stoichiometry; mini-ferritin.

INTRODUCTION

Deinococcus radiodurans has a remarkable ability to withstand challenging environments in which it is exposed to nutritional stress, ionizing radiation, oxidation, or other agents with the potential to damage cellular components.[1] Much emphasis has been placed on understanding how *D. radiodurans* repairs DNA breaks that would otherwise constitute irreversible and hence lethal damage to most microorganisms. Moreover, the existence of mechanisms that protect *D. radiodurans* from induced DNA damage have also been proposed, including its toroidal nucleoid structure and its high intracellular ratio of manganese to iron.[2–7]

DNA protection during starvation (Dps) proteins constitute another mechanism for preventing DNA damage. Since the discovery of Dps in *Escherichia coli*, where it is upregulated during stationary phase and in response to stress, Dps proteins from many bacterial species have been characterized.[8–14] A distinctive feature of Dps proteins is to prevent hydroxyl radical formation by ferroxidation and sequestration of iron, and several Dps proteins also bind nonspecifically to DNA.[15–17] DNA binding is usually associated with N- or C-terminal extensions preceding the conserved four-helix bundle subunits that assemble into a dodecameric sphere, the center of which harbors the distinctive iron core.[13,18,19]

Dps-1 is one of two homologs encoded by *D. radiodurans*.[19,20] The exact function of Dps-1 is still not known as it does not appear to sequester iron sufficiently avidly to avoid its spontaneous release from the protein core and subsequent participation in Fenton chemistry.[20,21] Its depletion also does not result in overt changes in *D. radiodurans* nucleoid structure.[22] Although a dimeric form of Dps-1 may be observed *in vitro*, the dodecameric assembly is highly favored[20]; we have previously shown that both dimeric and dodecameric Dps-1 bind DNA and that optimal binding interactions require 22-bp DNA. As DNA binding requires the N-terminal extensions interacting in DNA major grooves, a model for DNA binding was proposed in which DNA binds along the long axis of a Dps-1 dimer with N-terminal extensions from each monomer binding consecutive DNA major grooves.[19,20] As Dps-1 preferentially assembles into a dodecameric structure, its assembly from six dimers predicts a total of six possible DNA binding sites. We show here that

Abbreviations: Dps, DNA protection during starvation; EMSA, electrophoretic mobility shift assay; PMSF, phenyl methyl sulfonyl fluoride.

Khoa H. Nguyen and Luke T. Smith contributed equally to this work.
Luke T. Smith's current address is Department of Cell and Molecular Biology, University of Chicago, Chicago, IL 60637.
Grant sponsor: National Science Foundation; Grant numbers: MCB-0744240, MCB-1051610.
*Correspondence to: Anne Grove, Department of Biological Sciences, Louisiana State University, Baton Rouge, LA 70803. E-mail: agrove@lsu.edu.
Received 23 June 2011; Revised 30 September 2011; Accepted 6 October 2011
Published online 24 October 2011 in Wiley Online Library (wileyonlinelibrary.com). DOI: 10.1002/prot.23228

while dodecameric Dps-1 can bind six 22-bp DNA duplexes, the stoichiometry of binding to longer duplexes is lower, suggesting that two Dps-1 dodecamers may bind opposite faces of duplex DNA sufficiently long to present consecutive DNA major grooves on each face. Mutation of surface-exposed arginines maps the path of DNA relative to the N-terminal extensions. Combined with the ability of Dps-1 to prevent cyclization of DNA, these data suggest a model for interaction with chromosomal DNA.

MATERIALS AND METHODS

Mutagenesis, overexpression, and purification of Dps-1 and Dps-R

Wild-type Dps-1 was purified and characterized as described.[20] To introduce the Arg132Ser substitution into Dps-1, quick-change mutagenesis PCR was performed by whole plasmid amplification of pET5a carrying the *Dps-1 gene*. The following primers were used to introduce the mutation (CGC → AGC): 5′-GCC **AGC** TAC AGC ACC-3′ and 5′-GGT GCT GTA **GCT** GGC-3′ (mutated codon in boldface). The PCR product was transformed into *E. coli* TOP10 cells and the resulting plasmid confirmed by sequencing. The mutant Dps-1 (Dps-R) was overexpressed in *E. coli* BL21(DE3)pLysS using 1.0 m*M* isopropyl-β,D-thiogalactopyranoside for 2 h. Cells were lysed in lysis buffer [50 m*M* Tris, 0.25*M* NaCl, 5 m*M* Na_2EDTA, 5% glycerol, 5 m*M* β-mercaptoethanol, 0.1 m*M* phenylmethylsulfonyl fluoride (PMSF) and 0.5 mg/mL lysozyme], and cell lysates were dialyzed against buffer A [20 m*M* Tris-HCl (pH 7.5), 50 m*M* KCl, 5% glycerol, 1 m*M* EDTA, 5 m*M* β-mercaptoethanol, 0.2 m*M* PMSF] and applied to a heparin–agarose column equilibrated in buffer A. The protein was eluted with a linear gradient from 50 m*M* to 1*M* KCl in buffer A. Elutions from the heparin column containing the mutant protein were collected, dialyzed against buffer A, and applied to a diethylaminoethyl (DEAE)–Sepharose column equilibrated in buffer A and eluted with a linear gradient from 50 m*M* to 1*M* KCl in buffer A. Protein concentrations were determined by staining of SDS polyacrylamide gels with Coomassie brilliant blue, using bovine serum albumin (BSA) as a standard, and by using the Micro BCA Protein Assay Kit (Pierce). The absence of dimeric Dps-1 was confirmed by electrophoresis on 5% non-denaturing acrylamide gels. The gel recipe was the same as the running gel of SDS-PAGE according to Laemmli, excluding sodium dodecyl sulfate (SDS). The electrophoresis was carried out in 375 m*M* Tris-HCl, pH 8.7.

Electrophoretic mobility shift assays

Complementary synthetic oligonucleotides used to generate 22- and 26-bp DNA were purchased, and the concentrations were determined using their extinction coefficients by spectrometry on a SmartSpec 3000 spectrophotometer (BioRad). The sequences of 22- and 26-bp DNA (average G+C content) are 5′-GGACTACTATAAA TAGATGATC-3′ (22 bp) and 5′-CGTGACTACTATAAA TAGATGATCCG-3′ (26 bp). The top strand was ^{32}P-labeled at the 5′-end with phage T4 polynucleotide kinase. Equimolar amounts of complementary oligonucleotides were mixed, heated to 90°C, and cooled slowly to room temperature (23°C) to form duplex DNA.

Electrophoretic mobility shift assays (EMSA) were performed using 10% polyacrylamide gels [39:1 (w/w) acrylamide:bisacrylamide] in 0.5× TBE (50 m*M* Tris borate, 1 m*M* ethylenediaminetetraacetic acid (EDTA)). Gels were prerun for 30 min at 175 V at 23°C before loading the samples with the power on. For stoichiometry determinations, DNA and protein were incubated for 30 min at room temperature in binding buffer containing 20 m*M* Tris HCl (pH 8.0), 0.3*M* NaCl, 0.1 m*M* Na_2EDTA, 1 m*M* dithiothreitol, 0.05% Brij58, and 10 μg/mL of BSA (under these conditions, the K_d for Dps-1 binding to 22-bp DNA would be less than 0.5 n*M*, as the K_d of 0.5 n*M* was measured in a buffer containing not 0.3 but 0.5*M* NaCl).[19] Each reaction contained 100 fmol of DNA with increasing concentration of Dps-1 in a total reaction volume of 10 μL. For K_d determination of Dps-R, DNA and protein were incubated for 1 h at room temperature in binding buffer containing 200 m*M* Tris HCl (pH 8.0) and 500 m*M* NaCl (a 10-fold higher concentration of Tris compared with the stoichiometry measurements). Each reaction contained 5 fmol of DNA with increasing concentrations of Dps-1 or Dps-R in a total reaction of 10 μL. After electrophoresis, gels were dried and then protein–DNA complexes and free DNA were quantified by phosphorimaging, using software supplied by the manufacturer (ImageQuant 1.1). The region on the gel between complex and free DNA was considered as complex to account for complex dissociation during electrophoresis, and the fraction of bound DNA was calculated as the ratio of bound DNA to total counts in each lane. Total counts did not vary systematically as a function of protein concentration, indicating that recovery was independent of the extent of complex formation and that no material was selectively lost during handling. For K_d determination, the percentage of complex formation was plotted against [Dps] and data were fit to the Hill equation, $f = f_{max}\,[\mathrm{Dps}]^n/(K_d + [\mathrm{Dps}]^n)$, where f is fractional saturation, [Dps] is the protein concentration, K_d reflects the apparent equilibrium dissociation constant, and n is the Hill coefficient. For measurements of stoichiometry, the percentage of complex formation was plotted against [Dps-1]/[DNA] and fit to a smooth curve using the program KaleidaGraph. Tangents were generated from data points in the upward slope and in the plateau, and the stoichiometry of Dps-1 complex formation was extrapolated algebraically. Experiments were carried out at least

in triplicate, and several preparations of both DNA and proteins were used for which concentrations were independently determined. No differences between individual protein preparations were observed, and measured K_d values are consistent with initially reported values (provided identical buffer conditions).[19,20] Dps-1 is also very stable, as previously reported,[20] and no loss of activity (or dissociation of the dodecamer) was evident on storage.

Intrinsic fluorescence measurements

Fluorescence emission spectra from 280 to 500 nm were recorded on a Jasco FP-6300 spectrofluorimeter with an excitation wavelength of 280 nm at 23°C using a 0.5-cm path length cuvette. All experiments were performed with 0.03 mg/mL protein in 40 m*M* Tris-HCl (pH 8.0), 0.2 m*M* EDTA, 0.1% (w/v) Brij58, and 100 m*M* NaCl. Reactions were incubated at 23°C for 30 min before fluorescence was measured. The absorbance of each sample was measured from 280 to 500 nm to correct for the inner filter effect.[23]

The corrected protein fluorescence at each wavelength ($F_{corr}(\lambda)$) was obtained from the observed fluorescence by first correcting for the background fluorescence to obtain ($F_c(\lambda)$). Inner filter effects were then resolved by the following correction factor: $F_{corr}(\lambda) = F_c(\lambda) \times 10^{(A_{ex}/2+A_{em}/2)}$, where A_{ex} and A_{em} are the absorbances at the excitation and emission wavelengths, respectively.[23] $F_{corr}(\lambda)$ is only reported for samples in which both A_{ex} and A_{em} are less than 0.2. Fluorescence quenching (Q) on DNA binding was calculated by $Q = 1 - F_{corr}[X]/F_{corr}[0]$, where $F_{corr}[X]$ and $F_{corr}[0]$ are corrected fluorescence intensities with X μ*M* and 0 μ*M* DNA, respectively.

DNA cyclization

Plasmid pET5a was digested with BspHI to yield a 315-bp fragment, which was purified on a 2% agarose gel. The DNA fragment was ^{32}P-labeled at the 5′-end with phage T4 polynucleotide kinase. Ligase-mediated DNA cyclization experiments were carried out with varying protein concentrations. Reactions were initiated by the addition of T4 DNA ligase to a final volume of 10 μL. Reactions containing 1000 fmol DNA and the desired concentration of Dps-1 were incubated in 1× binding buffer with 200 m*M* NaCl and 1× ligase buffer (New England BioLabs, Ipswich, MA) at 23°C for 60 min. Formation of circular ligation product was confirmed by the addition of 1 μL of exonuclease III followed by 30-min incubation at 23°C. Reactions were terminated using 3 μL of 10% SDS followed by phenol-chloroform extraction and ethanol precipitation. Reactions were analyzed on a 8% polyacrylamide gel [39:1 (w/w) acrylamide:bisacrylamide] with 0.5× TBE as running buffer. After electrophoresis, gels were dried and ligation products were visualized by phosphorimaging.

Plasmid DNA ligation

Plasmid pET5a was linearized with EcoRI. Reactions were initiated by the addition of 200 U of T4 DNA ligase to a final volume of 10 μL. One hundred nanograms of DNA was incubated in 1× ligase buffer and 200 m*M* NaCl at room temperature for 60 min in the absence or presence of 1.3 pmol of Dps-1. Reactions were terminated with 10 μL of 75 m*M* EDTA, 6 mg/mL proteinase K, 15% glycerol, 1% SDS, bromophenol blue, and xylene cyanol, followed by a 30-min incubation at 55°C. Ligation products were resolved on 1% agarose gels in 0.5 × TBE buffer at 110 V for 2.5 h. Gels were stained with ethidium bromide.

RESULTS

Path of DNA relative to N-terminal extensions

Previous analyses of Dps-1 have shown that the N-terminal extension is important in DNA binding and that the main body of the protein contributes little to DNA binding in the absence of this extension.[19] Once DNA binding has been initiated, the DNA presumably interacts with the body of the protein; however, the exact path of DNA binding is still unknown. Looking at the structure of Dps-1, there is a single arginine residue that lies on the surface of Dps-1, in the short helix that connects the second and third helix of the four-helix bundle monomer, that has potential to interact with the DNA [Fig. 1(a,b)]. To specify the role of this residue in DNA binding, a mutant was constructed in which this residue is changed to a serine. EMSAs [Fig. 2(a,b)] show that this Dps-1 variant (Dps-R) binds DNA with lower affinity when compared with wild-type Dps-1. A complex is not apparent unless the DNA is incubated with 50 n*M* of Dps-R, and complexes are not stable and dissociate during electrophoresis; this results in saturation at a level of bound DNA that is much lower than total DNA. In contrast, essentially complete complex formation is seen with only 5 n*M* of Dps-1. Quantification of complex formation with Dps-1 yields a K_d of 4.0 ± 0.6 n*M* [Fig. 2(d)], which is about sixfold lower when compared with the mutant Dps-R [K_d = 24.0 ± 5.0 n*M*; Fig. 2(c)]. The K_d value for Dps-1 is higher than the previously reported K_d (~0.5 n*M*).[19] This is due to the higher ionic strength and different composition of the binding buffer when compared with that used for previous determinations. Altogether, these data suggest that Arg132 in the helix connecting helices 2 and 3 of the four-helix bundle monomer contributes to DNA binding. We also note that the modest positive cooperativity of binding seen here

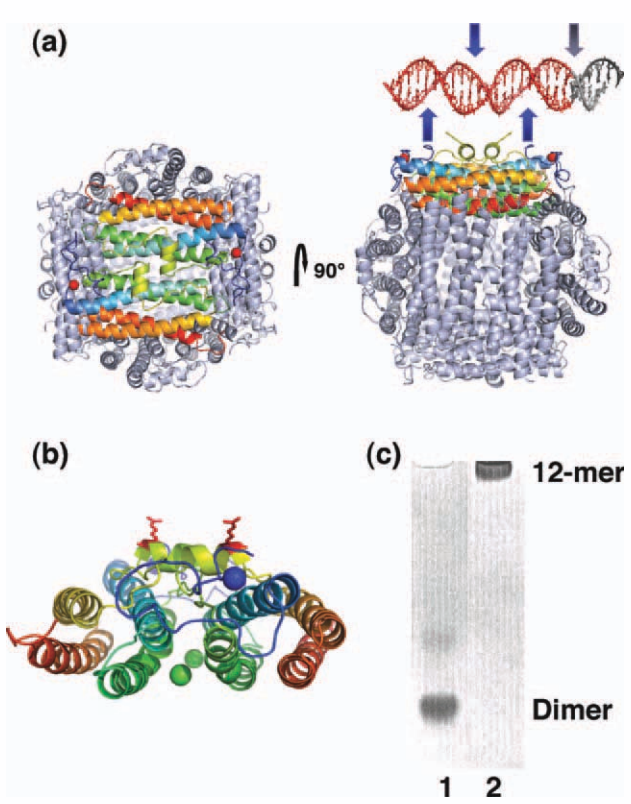

Figure 1

Possible DNA binding modes for dodecameric Dps-1. (**a**) The left side of the panel shows the structure of dodecameric Dps-1 (2F7N)[21] with a top view looking down on one of the six dimers [colored ribbons; blue to red starting at the N-terminus, with the short helices harboring R132 in yellow (perpendicular to the axis of the four-helix bundle)]. The red spheres represent cobalt. The right side of the panel shows a side view of the identified dimer, with R132 in stick representation (yellow). Each Dps-1 dimer binds two consecutive major grooves in duplex DNA, identified by blue arrows. For 22-bp DNA (shown as the red segment of the double helix), only one face of the helix presents two consecutive major grooves. For 26-bp DNA (the entire duplex segment, red and gray), there are potential binding sites on both faces of the duplex (identified by all arrows, blue and gray). (**b**) The Dps-1 dimer with each chain colored as above with R132 in red stick representation. Metal ions in the ferroxidase center located at the interface of two monomers are in green; metal ions at the N-terminal loops are in blue. (**c**) Native gel showing N-terminally truncated Dps-1 (dimer; Lane 1) and full-length Dps-1 (dodecamer; Lane 2). N-terminally truncated Dps-1 has been previously shown by both gel filtration and native gel electrophoresis to exist as a dimer, whereas full-length Dps-1 exists as a dodecamer.[19]

and previously reported for wild-type Dps-1 is lost on removal of Arg132.

Stoichiometric titrations reveal six DNA binding sites per Dps-1 dodecamer

The mode of DNA binding by dodecameric Dps-1 involves interaction of two metal-anchored N-terminal extensions in consecutive DNA major grooves, a binding mode in part inferred from the observation that Dps-1 exhibits optimal binding to 22-bp DNA, whereas interactions with shorter duplexes that do not present two consecutive DNA major grooves result in a significantly lower affinity.[19] Because Dps-1 dimers can bind DNA

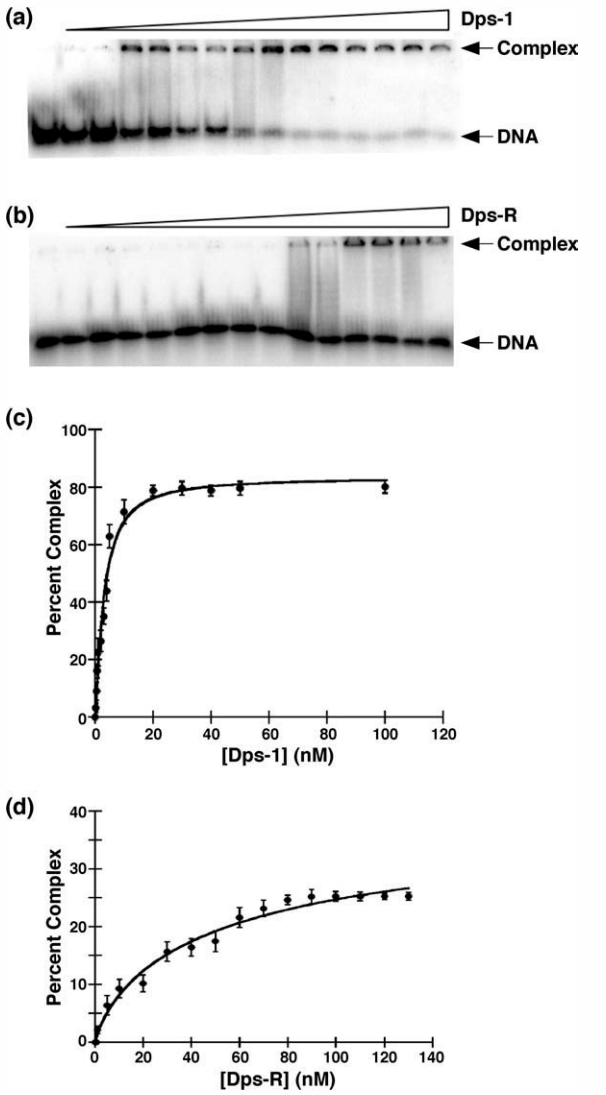

Figure 2

DNA binding by wild-type Dps-1 and Dps-R. Electrophoretic analysis of 26-bp duplex DNA titrated with Dps-1 (**a**) and Dps-R (**b**) under equilibrium conditions ([DNA] $< K_d$). Experiments with Dps-1 and Dps-R were performed side by side with the same DNA preparations. For Dps-1, concentrations are 0, 0.25, 0.5, 0.75, 1, 2, 3, 4, 5, 10, 20, 30, 40, 50, and 100 n*M*. For the mutant Dps-R, concentrations are 0, 0.25, 0.5, 1, 5, 10, 20, 30, 40, 50, 60, 70, 80, 90, and 100 n*M*. (**c**) Binding isotherm for Dps-1 binding to 26 bp (the presence of single-stranded DNA, to which Dps-1 does not bind, accounts for residual unbound DNA). (**d**) Binding isotherm for Dps-R binding to 26 bp (a larger fraction of DNA migrates at the position of the DNA reference band after incubation with Dps-R suggests that it derives from complexes that dissociated during electrophoresis and not from DNA species that are inactive for binding). The best fit to the data were obtained using the Hill equation ($R^2 = 0.9828$, $n = 1.3 \pm 0.2$ for Dps-1 and $R^2 = 0.9866$, $n = 0.8 \pm 0.1$ for Dps-R).

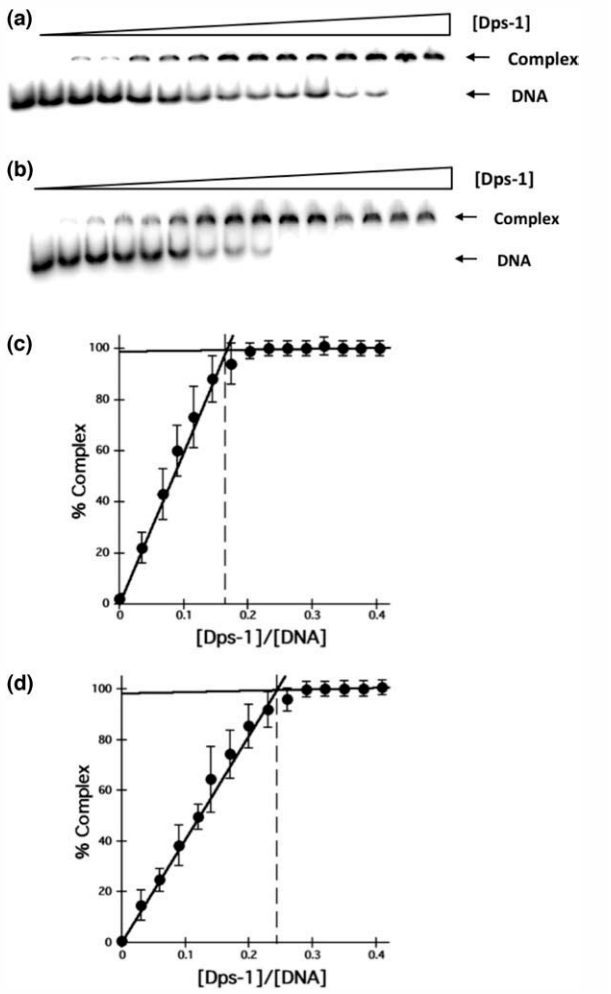

Figure 3

Stoichiometry of Dps-1 to DNA determined by electrophoretic mobility shift assays. (**a** and **b**) Stoichiometric titrations ([DNA] > K_d) of 100 fmol 22- and 26-bp DNA, respectively, with increasing concentrations of dodecameric Dps-1. Protein concentrations range from 0.15 to 2.1 n*M* for 22-bp DNA in increments of 0.15 n*M* and from 0.3 to 4.2 n*M* for 26-bp DNA in increments of 0.3 n*M*. Complex and free DNA are identified at the right. (**c** and **d**) Percent complex formation with 22- and 26-bp DNA, respectively, as a function of [Dps-1]/[DNA]. The intercepts of tangents to the upward slope and the saturation plateau reflect saturation. DNA preparations used in these experiments contain no single-stranded DNA.

and the Dps-1 dodecamer is assembled from six dimers, each Dps-1 dodecamer would have six potential binding sites for DNA. To assess this prediction, 22-bp DNA duplex was titrated with dodecameric Dps-1 under stoichiometric conditions ([DNA] > K_d), and complex formation was measured using EMSAs; under the solution conditions used, the DNA would be in at least 20-fold excess above the K_d. As shown in Figure 3, Dps-1 forms complexes with the DNA that are unable to enter the gel. When the percentage of complex formation was plotted against [Dps-1]/[DNA] and tangents were calculated from the upward slope and the saturation plateau, a break point was observed reflecting saturation of Dps-1 (Fig. 3). The 22-bp DNA was seen to saturate Dps-1 at a [Dps-1]/[DNA] ratio of 0.17:1, that is, a 5.9-fold molar excess of DNA is required to saturate the protein. This is consistent with the predicted existence of six DNA binding sites. We also note that dodecameric Dps-1 is the favored oligomeric assembly and that no dimer was detectable in the protein preparations used for this experiment [Fig. 1(c)]. Additionally, because an evaluation of stoichiometry requires knowledge of the active fraction of protein, we note the significant stability[20] of Dps-1 and the observation that no difference in activity is evident for different protein preparations or as a result of prolonged storage. The observed saturation of Dps-1 with a 5.9-fold molar excess of 22-bp DNA is consistent with expectations; indeed, it would be difficult to reconcile saturation at a higher ratio of DNA to protein with the assembly of Dps-1 from six dimers, each of which are capable of binding 22-bp DNA but not shorter duplexes.[20] Therefore, we have no indication that Dps-1 preparations are not essentially fully active.

As 22-bp DNA features two consecutive DNA major grooves only on one face of the DNA helix [Fig. 1(a)], a second Dps-1 protomer interacting with the opposite face of already bound DNA would be unfavorable.[19] Therefore, we investigated the stoichiometry of Dps-1 binding to 26-bp DNA that would be sufficiently long to feature consecutive major grooves on opposite faces of the duplex (Fig. 3). The rationale for this experimental design was that if two Dps-1 dodecamers cannot bind simultaneously to opposite faces of the duplex, then a 6:1 stoichiometry of DNA to Dps-1 should still be observed, whereas simultaneous Dps-1 binding to opposite DNA faces would result in a lower ratio of DNA to Dps-1 at saturation. As shown in Figure 3, 26-bp DNA duplex saturates Dps-1 at a [Dps-1]/[DNA] ratio of 0.24:1, that is, a 4.2-fold molar excess of DNA is required to saturate the protein, suggesting simultaneous binding of two Dps-1 dodecamers on either face of the 26-bp duplex.

Each Dps-1 monomer has two tryptophan residues; Trp84 at the end of α1 and Trp195 at the end of α4. An altered environment of tryptophan can be determined by changes in intrinsic fluorescence; therefore, we measured the change in intrinsic tryptophan fluorescence of Dps-1 on interaction with DNA to corroborate stoichiometry determinations by EMSA. The intrinsic fluorescence spectrum of dodecameric Dps-1 is characterized by an emission maximum at 330 nm and a shoulder at 338 nm on excitation at 280 nm (Fig. 4, black symbols). The most marked decrease in fluorescence is seen at a ratio of dodecameric Dps-1 to DNA of 1:1 (Fig. 4, blue diamond) with a further decrease in fluorescence with increasing amounts of DNA. Equimolar amounts of DNA and Dps-1 effectively shift the emission maximum

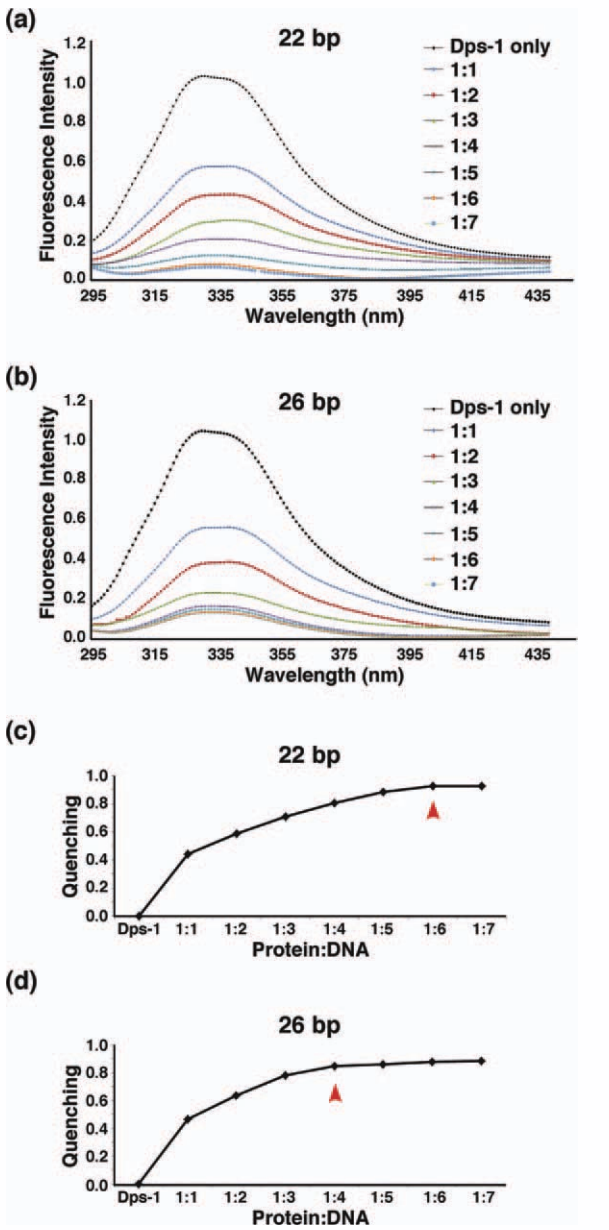

Figure 4

Stoichiometry of Dps-1 to DNA determined by quenching of intrinsic tryptophan fluorescence. (**a**) Intrinsic fluorescence of 0.03 mg/mL dodecameric Dps-1 titrated with 22-bp dsDNA (ratio of protein:DNA: blue diamond = 1:1; red square = 1:2; green triangle = 1:3; purple x = 1:4; turquoise x = 1:5; orange circle = 1:6; light blue square = 1:7; black symbol = Dps-1 only). (**b**) Intrinsic fluorescence of Dps-1 titrated with 26-bp dsDNA (protein:DNA: blue diamond = 1:1; red square = 1:2; green triangle = 1:3; purple x = 1:4; turquoise x = 1:5; orange circle = 1:6; light blue dot = 1:7; red dot with yellow line = Dps-1 only). (**c**) Intrinsic fluorescence quenching of dodecameric Dps-1 as a function of the concentration of 22-bp dsDNA. (**d**) Intrinsic fluorescence quenching of dodecameric Dps-1 as a function of the concentration of 26-bp dsDNA. Fluorescence quenching at peak fluorescence is graphically represented only for illustrative purposes.

to 339 nm by reducing the peak fluorescence at 330 nm to that of the shoulder to create one broad peak spanning from about 330 to 342 nm; with increasing [DNA], fluorescence intensity in decreased asymptotically, but the wavelength of peak intensity remains constant. Notably, effectively no further fluorescence quenching is observed across the entire spectrum beyond a DNA:Dps-1 ratio of 4:1 for 26-bp DNA [Fig. 4(b: purple symbols, d)], whereas fluorescence quenching on addition of 22-bp DNA continues until a ratio of 6:1 is reached [Fig. 4(a: orange symbols, c)]. These data suggest a different mode of binding of the two duplexes and are consistent with occupancy of six DNA binding sites by 22-bp DNA and with 26-bp DNA saturating Dps-1 at a lower stoichiometry. Although the roles of receptor and titrant are reversed in this experiment and equivalent stoichiometries of binding are suggested, we note that simultaneous binding of two Dps-1 dodecamers to one DNA duplex may affect fluorescence quenching.

Dps-1 restricts cyclization of short DNA fragments by T4 DNA ligase

The ability of Dps-1 to bend DNA was previously assessed using a cyclization assay in which DNA shorter than the persistence length was cyclized with T4 DNA ligase. Dps-1 was unable to promote cyclization of 105-bp DNA.[19] The proposed organization of DNA–Dps-1 complexes suggests that DNA will not wrap around a single dodecamer, consistent with the lack of cyclization observed with 105-bp DNA, and that Dps-1 will instead "stiffen" the DNA. This mode of DNA–Dps-1 interaction should prevent cyclization of longer DNA duplexes. Therefore, a ligase-mediated cyclization assay was performed with a longer 315-bp DNA, which can cyclize in the presence of T4 DNA ligase without the help of any DNA bending protein. As shown in Figure 5, 315-bp DNA can form minicircles in the absence of Dps-1; the addition of ~1 n*M* Dps-1 results in significantly reduced yield of circular ligation product, while linear dimer may still be seen (Lane 5), and higher concentrations of Dps-1 also inhibit the formation of linear dimer (Lanes 6 and 7). This is consistent with the interpretation that Dps-1 increases the persistence length at Dps-1 concentrations at which binding to multiple duplexes may not be the prevailing mode of binding; however, the experiment also suggests that Dps-1 produces DNA complexes at higher concentrations that resist multimer formation. This may be related to the binding of multiple DNA molecules per Dps-1 dodecamer that preclude proper alignment of DNA ends for ligation, as such duplexes would be bound at sites that are either at right angles to each other or at opposite faces of the dodecamer. This experiment also addresses the possibility that Dps-1 binds with significantly higher affinity to DNA ends when compared with internal sites; such binding modes would have been

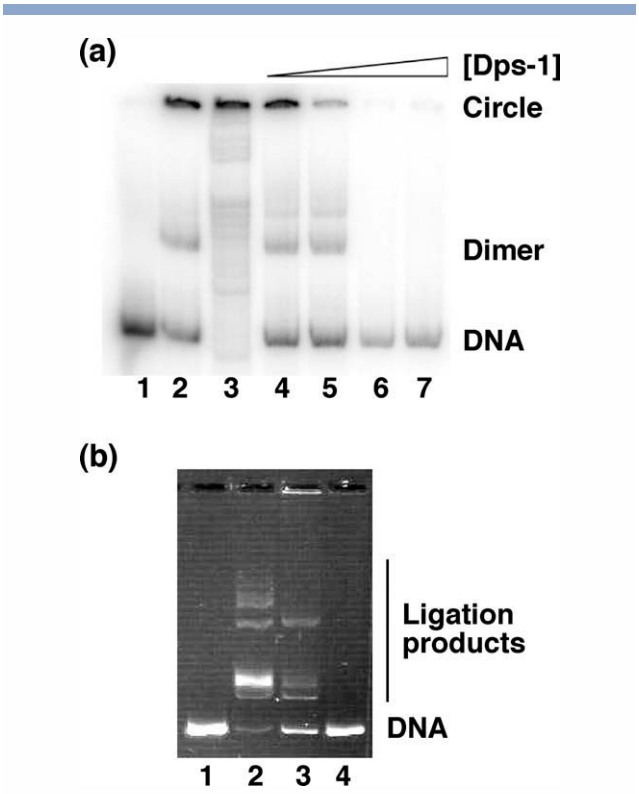

Figure 5

DNA end joining in the presence of Dps-1. (**a**) Dps-1 inhibits cyclization of 315-bp duplex DNA by T4 DNA ligase. Lane 1, 315-bp DNA alone. Lane 2, DNA and ligase. Lane 3, DNA, ligase, and exonuclease III. Lanes 4–7 show DNA incubated with ligase and increasing concentrations (0.8, 2.4, 8.0, and 24 ng) dodecameric Dps-1. Linear and circular ligation products are identified at the right. (**b**) Ligation of linearized plasmid DNA in the presence of Dps-1. Lane 1, linearized pET5a without the ligase. Lane 2, DNA after ligation in the absence of Dps-1. Lane 3, DNA after ligation in the presence of 1.3 pmol of Dps-1. Lane 4, DNA and Dps-1 in the absence of ligase.

expected to result in the inhibition of DNA ligation at a Dps-1 concentration that would be sufficient to saturate DNA ends. This is not observed as ligation of linearized plasmid pET5a by T4 DNA ligase was not inhibited by the addition of 1.3 pmol of Dps-1, which is more than sufficient to saturate the free DNA ends [130 n*M* protein, each featuring multiple DNA binding sites, to 7.6 n*M* DNA ends; Fig. 5(b), Lane 3]. Dps-1 binds dsDNA with very high affinity to internal sites ($K_d \sim 0.5$ n*M* under the ionic conditions of this experiment). The concentration of internal sites is much greater than the concentration of DNA ends (4134-bp plasmid featuring 188 contiguous 22 bp sites corresponding to 714 n*M* sites at saturation); assuming four DNA sites per Dps-1 dodecamer, 130 n*M* protein would feature 520 n*M* DNA binding site, comparable with the number of internal sites in the DNA. Therefore, this experiment suggests that Dps-1 does not prevent ligation by preferentially binding to the DNA ends or simply by interfering with ligase function.

DISCUSSION

The DNA binding site

DNA binding by Dps proteins generally requires extensions beyond the four-helix bundle core. Dps-1 is no exception; truncation of the N-terminal extensions has been previously shown to result not only in a lack of DNA binding but also in a failure to assemble into a dodecamer.[19] As high-affinity binding is observed only with DNA of sufficient length to feature two DNA major grooves on one face of the helix and as Dps-1 dimers retain the ability to bind DNA, DNA binding may entail N-terminal extensions from each monomer of a Dps-1 dimer occupying consecutive DNA major grooves. Such binding modes would align the DNA helix axis with the long axis of a Dps-1 dimer [Fig. 1(a)]. The surface-exposed helices α2 and α3 of the four-helix bundle monomer are connected by a short helix featuring Arg132, and further support of the proposed binding model is provided by the reduced DNA binding characteristic of a Dps-1 variant in which this residue is mutated (Fig. 2).

An explicit prediction from this binding model is that each Dps-1 dodecamer, which may be viewed as assembled from six dimers, should feature six binding sites and that adjacent sites should be at right angles to each other, thus precluding DNA wrapping about the protein surface. These predictions are borne out by experiment: the stoichiometry of 22-bp DNA to dodecameric Dps-1 is 6:1 (Figs. 3 and 4) and DNA binding by Dps-1 may increase its persistence length, as evidenced by attenuated DNA cyclization by T4 DNA ligase at low concentrations of Dps-1 [Fig. 5(a)] and by the previously observed failure of Dps-1 to promote cyclization of shorter duplexes.[19] Altogether, these data suggest that the DNA binding site in Dps-1 consists of N-terminal extensions from either monomer of a Dps-1 dimer and arginine residues in the loops connecting helices 2 and 3 and that Dps-1 features six such sites.

A change in intrinsic tryptophan fluorescence signals an altered environment. In Dps-1, Trp84 is at the end of α1, contributing to the dimer interface, and Trp195 is at the end of α4. This helix leads to a loop in which Arg205 contributes to coordinating a metal ion at the predicted iron exit pore.[21] As neither tryptophan would be predicted to contact DNA directly, an altered environment of one or both of these residues may arise due to a propagation of conformational changes on DNA binding. This is consistent with the observation that the greatest change in fluorescence quenching is seen at low DNA occupancy (Fig. 4), with the observed positive cooperativity of DNA binding of dodecameric Dps-1, and with the observation that dimeric Dps-1 does not bind DNA cooperatively.[19,20] In addition to the differential change in tryptophan fluorescence observed at different levels of DNA saturation, there is no reason to expect both

tryptophan residues to respond equivalently to conformational changes induced on DNA binding. These caveats notwithstanding, this experiment is consistent with the stoichiometries measured by EMSA.

Proposed model for Dps-1 binding to chromosomal DNA

The packing of *E. coli* Dps dodecamers in the crystal is approximately hexagonal.[24] Likewise, hexagonal packing was seen in electron micrographs of isolated Dps.[25] Although the addition of DNA did not affect the in-plane lattice spacing, it caused the rapid formation of sheet-like crystals, leading to the proposal that Dps coordinates DNA in alternating layers of protein and DNA.[5,25,26] In such layers, the DNA would be buried and thus physically protected from damage. Our data further supports and extends this model: Combining the stoichiometry data with the observation that Dps-1 "stiffens" DNA as well as the hexagonal packing of *E. coli* Dps dodecamers observed in the crystal and the layered appearance of *E. coli* Dps with DNA observed in electron micrographs, we propose that Dps-1 can bind DNA along the axis of each of six dimers [Fig. 1(a: 22-bp DNA illustrated in red)]. Two Dps-1 protomers can bind simultaneously to opposite faces of a duplex, provided that it is sufficiently long and can present two consecutive major grooves, as illustrated for 26-bp DNA [Fig. 1(a: 26-bp DNA includes gray extension)]. Our binding model is consistent with a hexagonal packing of Dps-1 dodecamers and with a layered appearance in complex with genomic DNA, as simultaneous binding to opposite faces of a DNA duplex would require each "layer" of Dps-1 dodecamers to fit into a knobs-into-holes type arrangement with DNA passing between each Dps-1 layer [Fig. 6(a: DNA illustrated as red cylinders)]. According to this model, two of the six possible DNA binding sites per dodecamer would be occupied [Fig. 6(a: rainbow-colored dimers along the *x*-axis, b: blue and green dimers)]. Notably, our data also suggest that the direction of DNA potentially bound at the remaining four sites would have to follow right angles relative to the sites parallel to the *x*-axis. Because sites parallel to the *y*-axis [Fig. 6(a: gray dimers, b: orange and purple dimers)] are not aligned between Dps-1 dodecamers in adjacent layers, DNA binding along the *y*-axis is likely unfavorable. In contrast, further pseudo-hexagonal packing along the *z*-axis would align binding sites from dodecamers in adjacent layers [Fig. 6(a: blue dimers parallel to the *z*-axis, b: red and yellow dimers)], potentially allowing DNA duplexes to bind along the *z*-axis, further reinforcing the sheet-like packing, and allowing a maximal occupancy of four of six potential DNA binding sites per dodecamer. Such highly ordered assemblies would allow packing of the otherwise flexible DNA into the crystalline structures observed under conditions that promote upregulation of Dps.

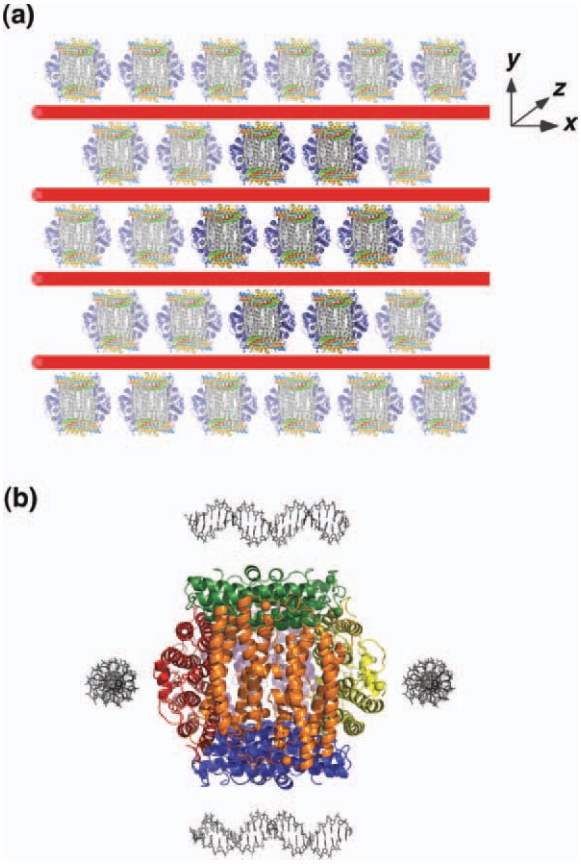

Figure 6

Model of dodecameric Dps-1 binding to genomic DNA. (**a**) A hexagonal arrangement of Dps-1 dodecamers with DNA (red cylinders) bound along the *x*-axes. (**b**) Dps-1 dodecamer with each dimer in a different color; DNA binds along the horizontal *x*-axis to blue and green dimers (top and bottom) with the DNA helix axis parallel to that of the four-helix bundle and along the *z*-axis to red and yellow dimers (left and right).

Bacterial nucleoids are compacted by association with proteins such as HU (whose name derives from histone-like and the U93 strain of E. coli from which it was first isolated), integration host factor (IHF), histone-like nucleoid-structuring (H-NS), factor for inversion stimulation (Fis), and Dps that either promote and constrain DNA supercoiling or bridge distant DNA segments.[27,28] In *E. coli*, Dps is upregulated in stationary phase and is central to cellular stress responses.[8,9] Under such circumstances, the ability to bridge DNA by the association of each Dps protomer with multiple DNA segments is likely the key to the observed DNA compaction and the formation of the crystalline arrays observed under severe stress conditions.[25,26] In *D. radiodurans*, the function of Dps-1 is less clear; although *D. radiodurans* does not encode homologs of many of the nucleoid-associated proteins characterized in *E. coli*, deletion of Dps-1 does not appear to cause overt changes in nucleoid morphology in

exponential or early stationary phase cells as evidenced by DAPI staining of the nucleoids (with the caveat that other nucleoid-associated proteins such as HU may be upregulated to compensate for the loss of Dps-1).[22] However, it remains to be determined if *D. radiodurans* Dps-1 is likewise upregulated under the severe stress conditions under which *E. coli* Dps induces the formation of DNA-protective crystalline arrays.

ACKNOWLEDGMENTS

The authors thank Dr. Marcia Newcomer for the use of the spectrofluorimeter.

REFERENCES

1. Cox MM, Keck JL, Battista JR. Rising from the ashes: DNA repair in *Deinococcus radiodurans*. PLoS Genet 2010;6:e1000815.
2. Levin-Zaidman S, Englander J, Shimoni E, Sharma AK, Minton KW, Minsky A. Ringlike structure of the *Deinococcus radiodurans* genome: a key to radioresistance? Science 2003;299:254–256.
3. Daly MJ, Gaidamakova EK, Matrosova VY, Vasilenko A, Zhai M, Leapman RD, Lai B, Ravel B, Li SM, Kemner KM, Fredrickson JK. Protein oxidation implicated as the primary determinant of bacterial radioresistance. PLoS Biol 2007;5:e92.
4. Zimmerman JM, Battista JR. A ring-like nucleoid is not necessary for radioresistance in the Deinococcaceae. BMC Microbiol 2005; 5:17.
5. Frenkiel-Krispin D, Ben-Avraham I, Englander J, Shimoni E, Wolf SG, Minsky A. Nucleoid restructuring in stationary-state bacteria. Mol Microbiol 2004;51:395–405.
6. Slade D, Radman M. Oxidative stress resistance in *Deinococcus radiodurans*. Microbiol Mol Biol Rev 2011;75:133–191.
7. Fredrickson JK, Li SM, Gaidamakova EK, Matrosova VY, Zhai M, Sulloway HM, Scholten JC, Brown MG, Balkwill DL, Daly MJ. Protein oxidation: key to bacterial desiccation resistance? ISME J 2008;2:393–403.
8. Almirón M, Link AJ, Furlong D, Kolter R. A novel DNA-binding protein with regulatory and protective roles in starved *Escherichia coli*. Genes Dev 1992;6:2646–2654.
9. Martinez A, Kolter R. Protection of DNA during oxidative stress by the nonspecific DNA-binding protein Dps. J Bacteriology 1997;179: 5188–5194.
10. Bozzi M, Mignogna G, Stefanini S, Barra D, Longhi C, Piera V, Chiancone E. A novel non-heme iron-binding ferritin related to the DNA-binding proteins of the Dps family *Listeria innocua*. J Biol Chem 1996;272:3259–3265.
11. Papinutto E, Dundon WG, Pitulis N, Battistutta R, Montecucco C, Zanotti G. Structure of two iron-binding proteins from *Bacillus anthracis*. J Biol Chem 2002;277:15093–15098.
12. Halsey TA, Vazquez-Torres A, Gravdahl DJ, Fang FC, Libby SJ. The ferritin-like Dps protein is required for *Salmonella enterica* serovar typhimurium oxidative stress resistance and virulence. Infect Immun 2004;72:1155–1158.
13. Ceci P, Mangiarotti L, Rivetti C, Chiancone E. The neutrophil-activating Dps protein of *Helicobacter pylori*, HP-NAP, adopts a mechanism different from *Escherichia coli* Dps to bind and condense DNA. Nucleic Acids Res 2007;35:2247–2256.
14. Liu X, Kim K, Leighton T, Theil EC. Paired *Bacillus anthracis* Dps (mini-ferritin) have different reactivities with peroxide. J Biol Chem 2006;281:27827–27835.
15. Zhao G, Ceci P, Ilari A, Giangiacomo L, Laue TM, Chiancone E, Chasteen ND. Iron and hydrogen peroxide detoxification properties of DNA-binding protein from starved cells. J Biol Chem 2002;277: 27689–27696.
16. Ilari A, Ceci P, Ferrari D, Rosse GL, Chiancone E. Iron incorporated into *Escherichia coli* Dps gives rise to a ferritin-like microcrystalline core. J Biol Chem 2002;277:37619–37623.
17. Pulliainen AT, Haataja S, Kähkönen S, Finne J. Molecular basis of H_2O_2 resistance mediated by Streptococcal Dpr. Demonstration of the functional involvement of the putative ferroxidase center by site-directed mutagenesis in *Streptococcus suis*. J Biol Chem 2003; 278:7996–8005.
18. Stillman TJ, Upadhyay M, Norte VA, Sedelnikova SE, Carradus M, Tzokov S, Bullough PA, Shearman CA, Gasson MJ, Williams CH, Artymiuk PJ, Green J. The crystal structures of *Lactococcus lactis* MG1363 Dps proteins reveal the presence of an N-terminal helix that is required for DNA binding. Mol Microbiol 2005;57:1101–1112.
19. Bhattacharyya G, Grove A. The N-terminal extensions of *Deinococcus radiodurans* Dps-1 mediated DNA major groove interactions as well as assembly of the dodecamer. J Biol Chem 2007;282:11921–11930.
20. Grove A, Wilkinson S. Differential DNA binding and protection by dimeric and dodecameric forms of the ferritin homolog Dps from *Deinococcus radiodurans*. J Mol Biol 2005;347:495–508.
21. Kim SG, Bhattacharyya G, Grove A, Lee YH. Crystal structure of Dps-1, a functionally distinct Dps protein from *Deinococcus radiodurans*. J Mol Biol 2006;361:105–114.
22. Nguyen HH, de la Tour CB, Toueille M, Vannier F, Sommer S, Servant P. The essential histone-like protein HU plays a major role in *Deinococcus radiodurans* nucleoid compaction. Mol Microbiol 2009;73:240–252.
23. Carpenter ML, Oliver AW, Kneale GG. Analysis of DNA-protein interactions by intrinsic fluorescence. Methods Mol Biol 2001;148: 491–502.
24. Grant RA, Filman DJ, Finkel SE, Kolter R, Hogle JM. The crystal structure of Dps, a ferritin homolog that binds and protects DNA. Nat Struct Biol 1998;5:294–303.
25. Wolf SG, Frenkiel D, Arad T, Finkel SE, Kolter R, Minsky A. DNA protection by stress-induced biocrystallization. Nature 1999;400:83–85.
26. Frenkiel-Krispin D, Minsky A. Nucleoid organization and the maintenance of DNA integrity in *E. coli*, *B. subtilis* and *D. radiodurans*. J Struct Biol 2006;156:311–319.
27. Dorman CJ. Nucleoid-associated proteins and bacterial physiology. Adv Appl Microbiol 2009;67:47–64.
28. Grove A. Functional evolution of bacterial histone-like HU proteins. Curr Issues Mol Biol 2011;13:1–12.